



Research article

Synthesis, characterization, and biological evaluation of novel cinnamic acid derivatives: cinnamoyl-metronidazole ester and cinnamoyl-memantine amide

Mohammad Moatz Shollar^a, Joumaa Merza^{a,b}, Maher Darwish^{c,*},
Mohammad Keshe^a^a Department of Chemistry, Faculty of Science, Al-Baath University, Homs, Syria^b School of Pharmacy, Faculty of Medical Sciences, Newcastle University, King George VI Building, Newcastle Upon Tyne, NE1 7RU, UK^c Department of Pharmaceutical Chemistry and Drug Control, Faculty of Pharmacy, Wadi International University, Homs, Syria

ARTICLE INFO

Keywords:

Cinnamic acid
Cinnamoyl chloride
Memantine
Metronidazole
Antibacterial
Antifungal

ABSTRACT

In this study, two derivatives, namely the ester derivative cinnamoyl metronidazole and the amide derivative cinnamoyl memantine, were synthesized from cinnamic acid and respective drugs for the purpose of exploring their potential as novel and efficient antimicrobial agents in the quest of prevailing the global antimicrobial resistance challenge.

The synthesis process involved two steps: first, the chlorination of cinnamic acid using thionyl chloride, and second, the esterification of metronidazole or the amidation of memantine. These steps resulted in the formation of cinnamoyl metronidazole/memantine. Optimal reaction conditions were established, and chromatographic techniques were used to separate the synthesized compounds. Confirmation of successful synthesis was achieved through FT-IR analysis, which readily distinguished the chlorinated product and derivatives based on distinctive bands, including mainly the one of carbonyl group. Additionally, molecular structures were validated using ¹H NMR and ¹³C NMR, with all peaks further confirming the successful esterification/amidation of cinnamoyl and drug moieties.

Upon evaluating the biological activity, the parent compounds exhibited negligible effects within the tested concentration range. However, the derivatives demonstrated significant activity. The ester derivative exhibited potent activity against the Gram-positive bacterium *Staphylococcus aureus*, as evidenced by a zone of inhibition measuring 12–15 mm in diameter. Conversely, the amide derivative displayed appreciable biological activity against *Candida* fungi, with an inhibition zone measuring 11–14 mm.

1. Introduction

The field of synthetic pharmaceutical derivatives has gained significant importance among researchers in their pursuit of developing compounds with high medical efficacy and minimal side effects. This endeavor aims to combat numerous epidemics and stubborn diseases on one hand and harness economic benefits on the other [1]. One of the primary methods for synthesizing these

* Corresponding author.

E-mail addresses: shollar.com@hotmail.com (M.M. Shollar), mjoma10@yahoo.com (J. Merza), darwish_maher@ymail.com, maherdarwish@wiu.edu.sy (M. Darwish), mohammad.keshe@gmail.com (M. Keshe).

<https://doi.org/10.1016/j.heliyon.2024.e29851>

Received 17 January 2024; Received in revised form 11 April 2024; Accepted 16 April 2024

Available online 21 April 2024

2405-8440/© 2024 The Author(s). Published by Elsevier Ltd. This is an open access article under the CC BY-NC license (<http://creativecommons.org/licenses/by-nc/4.0/>).

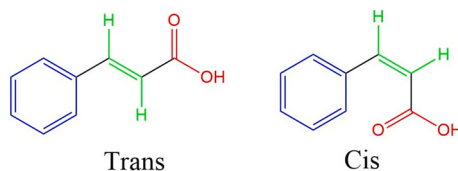


Fig. 1. Geometric isomerism of CA.

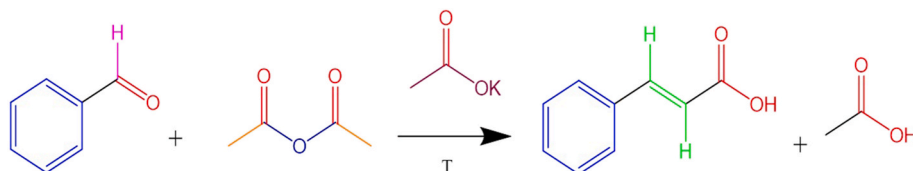


Fig. 2. Preparation of CA via the Perkin reaction.

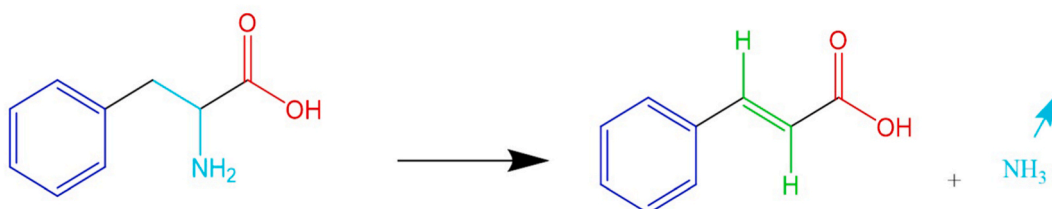


Fig. 3. Synthesis of CA from phenylalanine.

derivatives involves their preparation from simple chemical compounds readily available in their commercial forms, using a series of chemical reactions spanning multiple stages. Alternatively, it involves modifying the structure of certain pharmaceutical and non-pharmaceutical compounds, allowing the generation of new derivatives with important properties and applications. This approach achieves the desired objectives by reducing production stages and increasing efficiency [2]. Either way, new derivatives formation is considered a challenge, as there is no uniform method for synthesizing them all. This process relies on assessing the biological effectiveness and physical properties of the compounds to be used as starting materials. After identifying and analyzing the data and characteristics of the manufactured compounds, the biological testing phase is initiated [3,4].

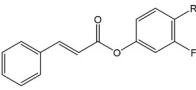
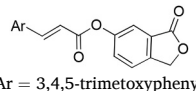
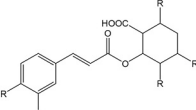
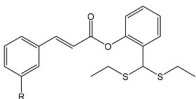
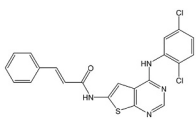
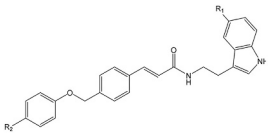
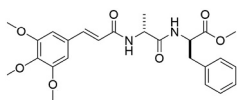
Cinnamic acid (CA), a natural compound with an unsaturated bond (Fig. 1), has gained prominence due to its diverse pharmacological properties, including anti-inflammatory, antimicrobial, and antifungal activities. What makes CA unique is its structure composed of three active centers (carboxylic group, double bond, and aromatic benzene ring) [5]. These structural features make it of great significance in synthesizing derivatives that have shown notable effects in reducing reactive oxygen species and proinflammatory cytokines and have a stronger efficacy against various ailments and sustainable diseases such as neurodegenerative disorders like Alzheimer's, advanced stages of diabetes, and malignant tumors [6,7]. Due to its significance and increasing commercial demand, it became necessary to synthesize CA rather than extract it in limited quantities. The majority of CA synthesis involves the condensation of benzaldehyde with several compounds using the Perkin Reaction [8]. These compounds include acetyl chloride, acetic anhydride, and malonic acid, according to the following reaction (Fig. 2). It can also be synthesized by removing the amino group from the compound phenylalanine [9], using the following reaction (Fig. 3).

Even though CA is proven to have antimicrobial activity against many pathogens, its limited water solubility hinders its use as a bare compound [10]. In the face of this challenge and others such as drug resistance and the need for effective therapies with low adverse side effects, the development of therapeutic compounds based on CA derivatives has emerged as a promising avenue of research. Several CA derivatives that have demonstrated efficacy, showcasing the compound versatile applications are reported in Table 1.

Metronidazole, an antibiotic characterized by a 5-nitroimidazole chemical structure, is extensively employed as an antibacterial and antiparasitic agent due to its efficacy and reliability. Despite its effectiveness in treating giardiasis, its utility is constrained in pediatric cases, and the emergence of drug-resistant strains poses limitations. Metronidazole, a prominent drug for over five decades, has found applications both topically and systemically [17]. Nevertheless, there remains a scarcity of comprehensive information regarding its potential in derivative formulas such as with CA.

Moreover, memantine (3,5-dimethyladamantane-1-amine) is a derivative of adamantane and is utilized as a medication in the treatment of Alzheimer's disease. It has been validated as an effective inhibitor of the M_2 ion channel of the influenza virus. Furthermore, the designed derivatives of memantine have demonstrated antimicrobial activity [18].

Table 1
Some CA derivatives with their structures and biological activities.

Derivative	Formula	Significance	Ref
3-fluoro-4-R-phenyl cinnamate		Antifungal	[11]
(E)-3-oxo-1,3-dihydroisobenzofuran-5-yl-(3,4,5-trimethoxy) cinnamate	Ar = 3,4,5-trimethoxyphenyl 	Anti-leishmania	[12]
Chlorogenic acid		Antibacterial Anti-virus (HSV-1 & HSV2)	[13]
2-(bis(ethylthio) R)phenyl (E)-3-(m-tolyl)acrylate		Anti-tuberculosis	[14]
N-(4-((2,5-dichlorophenyl)amino)thieno[2,3-d]pyrimidin-6-yl)cinnamamide		Anti-cancer	[15]
(E)-N-(2-(5-R ₁ -1H-indol-3-yl)ethyl)-3-(4-((p-tolyl)oxy)R ₂)phenyl)acrylamide		Alzheimer's disease	[16]
Methyl-((E)-3-(3,4,5-trimethoxyphenyl)acryloyl)-d-alanyl-d-phenylalanin-eate		Alzheimer's disease	[7]

In our study, we focus on synthesizing two new derivatives, cinnamoyl metronidazole (C-MET) and cinnamoyl memantine (C-MEM), starting from CA and pharmaceutical compounds metronidazole and memantine, respectively. These derivatives were rigorously evaluated for their antibacterial and antifungal efficacy against the Gram-positive bacterium *Staphylococcus aureus*, Gram-negative bacterium *Pseudomonas aeruginosa*, and the fungus *Candida albicans*. Through this research, we aim to contribute to the growing body of knowledge concerning CA derivatives and their potential applications in medicine and related fields.

2. Materials and instrumentation

The chemicals used in the research include *trans*-CA, benzene, chloroform, memantine, metronidazole, dichloromethane, sodium bicarbonate, methanol, pyridine, ethyl ether, toluene, dimethyl sulfoxide, and thionyl chloride. These chemicals were sourced from reputable companies including Sigma-Aldrich, ChemLAB, Riedel-deHaen, and Merck BDH. All were analytical grade and used as received.

The instruments utilized include a 600 MHz Nuclear Magnetic Resonance (¹H NMR and ¹³C NMR) Spectrophotometer from JEOL, Japan, a 400 MHz Proton Nuclear Magnetic Resonance (¹H NMR) Spectrophotometer from Russia, a Fourier-Transform Infrared (FT-IR) Spectrophotometer Model FT-IR-4100 from Shimadzu, Japan, a Rotavapor Model 4.91 from Normschiff, Germany. Column chromatography was performed on 230–400 mesh silicagel (Kieselgel 60, Merck, Germany).

In all synthesis procedures, the progress of the reaction was monitored via Thin-Layer Chromatography (TLC) employing appropriate mobile phases. The TLC plates, composed of aluminum coated with silica gel 60F₂₅₄ measuring 20 × 20, were provided by Merck, Germany. Samples were periodically extracted using capillary tubes at 15 min intervals with continuous stirring. The formation of the desired product was confirmed by the appearance of new spots on the TLC plate, distinct from those of the initial reactants.

2.1. Synthesis of cinnamoyl metronidazole (C-MET)

The synthesis of C-MET involved a two-step process: initially synthesizing cinnamoyl chloride from CA and thionyl chloride,

Table 2
Reagents quantities for the synthesis of C-MEM.

Reagent	Amount (mL)
benzene	10
chloroform	5
acidic sodium bicarbonate 1 %	0.2
toluene	10
pyridine	0.05

followed by the formation of the ester derivative, cinnamoyl metronidazole, from cinnamoyl chloride and metronidazole. We explored two methodologies to optimize the yield.

2.1.1. Cinnamoyl chloride preparation

Cinnamoyl chloride was synthesized from CA using a modified procedure from Ref. [19]. Initially, 1 g CA was dissolved in 10 mL dichloromethane under magnetic stirring at room temperature in a three-neck flask. The solution was then cooled in an ice bath before adding 5 mL of thionyl chloride (SOCl₂) dropwise using a dropping funnel over 30 min, ensuring the reaction temperature did not exceed room temperature. After the initial reaction period, additional 3 mL of thionyl chloride was introduced over 15 min to complete the conversion. After removal from the ice bath, the solution was allowed to warm to ambient laboratory conditions under continuous stirring. Subsequently, the temperature was carefully increased to 50 °C, leading to the evolution of gases, specifically HCl and SO₂, which were safely diverted into a sodium hydroxide solution via a glass adapter to neutralize them. Concurrently, a noticeable transition in the reaction mixture color from yellow to orange-yellow signaled the successful formation of the desired product.

The reaction progress was monitored by TLC, with the mobile phase consisting of 75 % methanol and 25 % ethyl ether. The completion was indicated by the Rf values of cinnamic acid (0.69) and cinnamoyl chloride (0.81). The product was purified using a rotary evaporator, yielding needle-like cinnamoyl chloride crystals, characterized by a melting point of 35.3 °C and a high purity yield of 98 %.

2.1.2. Method 1 of C-MET preparation (C-MET)

In the preparation of C-MET, a round-bottom flask equipped with a dropping funnel was cooled in an ice bath. To this, 10 mL of benzene was added, followed by 0.17 g of metronidazole (1 mmol), stirred magnetically. Subsequently, 5 mL of chloroform containing 0.2 g of cinnamoyl chloride (1.2 mmol) was introduced dropwise over 30 min. The mixture was then allowed to reach room temperature with continuous stirring. Upon removal of the dropping funnel, a reflux condenser was attached, and the temperature was increased to benzene's boiling point. The reaction was maintained at this temperature for 1 h with stirring. Post-reaction, the mixture was treated dropwise with a 1 % acidic sodium bicarbonate aqueous solution, added four times to ensure complete quenching (0.3 mL in total). TLC monitoring was employed throughout, using a mobile phase of 50 % methanol, 45 % dichloromethane, and 5 % benzene, yielding Rf values for metronidazole (0.56), C-MET (0.14), and cinnamoyl chloride (0.65).

After neutralization with 10 mL of sodium hydroxide solution, the reaction mixture separated into two distinct layers. The upper aqueous layer contained inorganic salts such as sodium chloride and the sodium salt derivative of CA, while the lower organic layer held the desired product, C-MET, along with any unreacted metronidazole. The layers were divided using a separating funnel. Subsequently, the organic phase was concentrated via rotary evaporation. The compounds were then isolated through column chromatography, employing a mobile phase of 50 % methanol, 45 % dichloromethane, and 5 % benzene. This process yielded a yellowish-white solid identified as C-MET, with a melting point range of (115.4–116) °C and a synthesis yield of 78 %.

2.1.3. Method 2 of C-MET preparation (C-MET)

In the synthesis, a round-bottom flask containing 10 mL of toluene was cooled in an ice bath. Metronidazole (0.17 g) was added, followed by a dropwise addition of 0.2 g of cinnamoyl chloride in 5 mL of toluene over 30 min. The reaction was stirred until it reached room temperature, then heated to 110 °C with a reverse condenser. Pyridine (0.05 mL) was added twice at 1-h intervals and turbidity observed. TLC monitoring used a mobile phase from method 1, with Rf values for metronidazole (0.56), C-MET (0.14), and cinnamoyl chloride (0.65). The mixture was then treated with 10 mL of double-distilled water, forming two layers. The organic layer, containing C-MET and unreacted metronidazole, was separated and washed with 10 mL of alkaline water. After evaporation, the compounds were isolated by column chromatography, yielding C-MET as a white to pale yellow solid, melting at (115.4–116) °C, with a 84 % yield.

2.2. Synthesis of cinnamoyl memantine (C-MEM)

The amide derivative C-MEM was synthesized from cinnamoyl chloride and memantine using two distinct methods, paralleling the C-MET synthesis with minor modifications. Specifically, in method 1, the NaHCO₃ solution was added in two instalments. Detailed quantities of reagents utilized in the synthesis are tabulated in Table 2.

The TLC and column chromatography were conducted using a mobile phase composed of 75 % isopropanol and 25 % benzene. The synthesis culminated in the formation of a white powder, identified as C-MEM, with a melting point of (201) °C. The yields were 88 % with method 1 and method 2 slightly higher at 90 %.

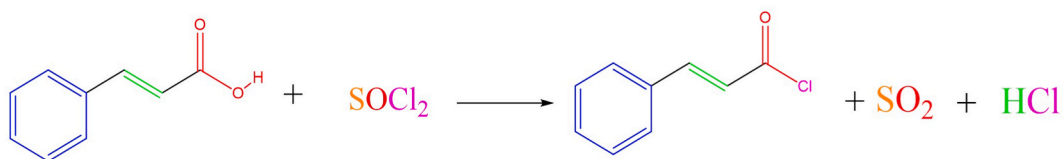


Fig. 4. Preparation of cinnamoyl chloride.

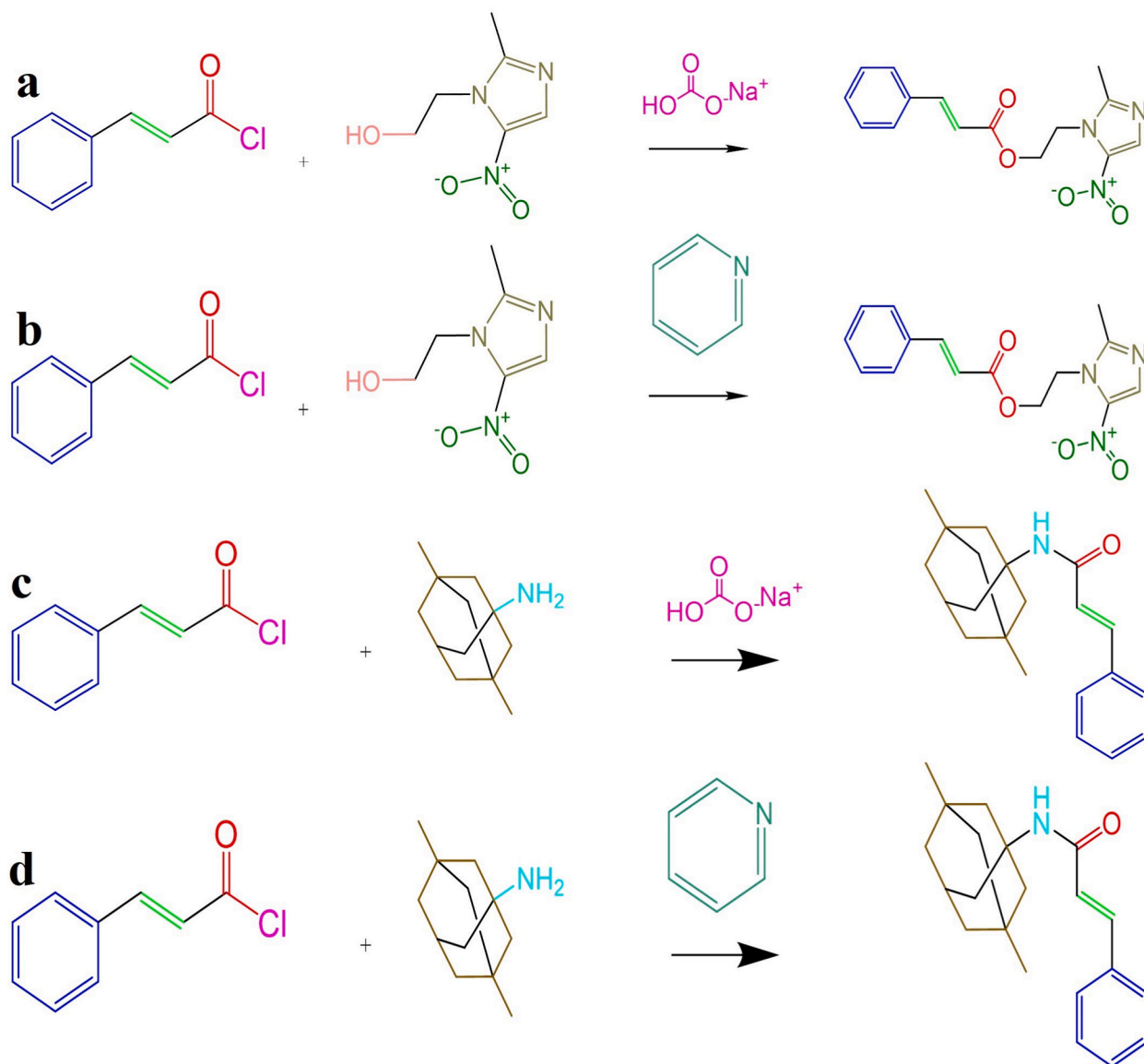


Fig. 5. Synthesis of compounds C-MET (a,b) and C-MEM (c,d) according to the first and second methods, respectively.

2.3. Biological activity tests

The *in vitro* antibacterial and antifungal activities of samples were evaluated using the agar diffusion method. Briefly, sample solutions of metronidazole, memantine, CA, C-MET, and C-MEM were prepared at levels of 100 and 200 $\mu\text{g mL}^{-1}$, along with the reference substance (gentamicin, GE and clotrimazole, CLO) at a concentration of 100 $\mu\text{g mL}^{-1}$, using dimethyl sulfoxide (DMSO) as the solvent.

For the antibacterial activity test, the Gram-positive bacteria (*Staphylococcus aureus*) and Gram-negative bacteria (*Pseudomonas*

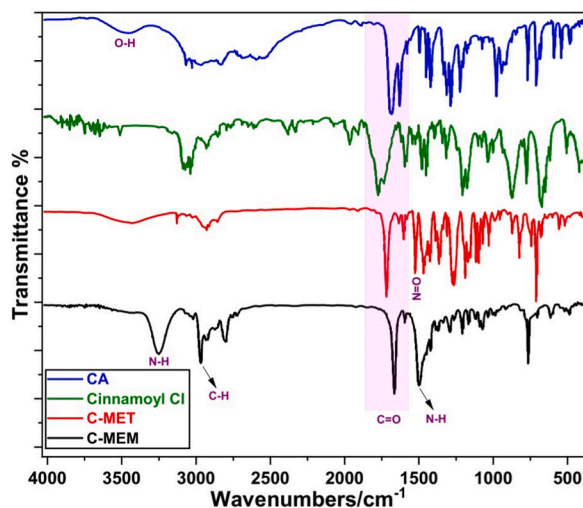


Fig. 6. FT-IR spectra of CA, cinnamoyl hydrochloride, and the derivatives.

aeruginosa) were first activated on tryptone soya bean broth for 24 h and then bacterial solutions were inoculated onto the tryptone soya bean agar poured in Petri dishes and evenly spread. Thereafter and by using stainless steel cylinders, 8 mm in diameter holes were made in the agar and loaded with 300 μL of the tested solutions. Finally, the dishes were incubated for 36 h at a temperature of 36.5–37 $^{\circ}\text{C}$.

For the antifungal activity assessment, samples were inoculated with *Candida Albicans* fungi in the agar nutrient medium and the dishes were then incubated for 48 h at a temperature of 25 ± 1 $^{\circ}\text{C}$ [20].

After incubation, the antimicrobial activity was assessed by observing the clear areas surrounding the wells. These clear areas were considered as zones of inhibition and their measurements were recorded in millimeters.

3. Results and discussion

3.1. Synthesis of C-MET

The synthetic routes for the novel CA ester and amide derivatives are outlined in Figs. 4 and 5. These compounds were all synthesized in two steps: the first one involved the formation of cinnamoyl chloride through the reaction of CA with thionyl chloride as represented in Fig. 4. Optimal reaction conditions for the best yield were keeping the reaction temperature below 5 $^{\circ}\text{C}$ until the laboratory temperature using an ice bath, the reaction time was 2–3 h.

The second step in the process for synthesizing the compounds C-MET and C-MEM was through a chemical reaction between metronidazole or memantine with cinnamoyl chloride. This was accomplished using two different processes that used sodium bicarbonate (Fig. 5a and c) and pyridine (Fig. 5b and d) as intermediates. The produced HCl from these reactions was then isolated to obtain the desired ester and amide. The optimal reaction conditions for the highest yields for both C-MET and C-MEM were 2 h at a reaction temperature of 80 $^{\circ}\text{C}$ and 2 h at a reaction temperature of 110 $^{\circ}\text{C}$ for the bicarbonate and pyridine methods, respectively. Furthermore, bicarbonate induced a higher yield than pyridine which was then adopted for further synthesis and characterization processes.

3.2. Molecular structure characterization

The molecular structure of the best yielded compounds, C-MET and C-MEM, was confirmed using ^1H NMR, ^{13}C NMR and FT-IR spectroscopic techniques.

3.2.1. FT-IR spectral analysis

FT-IR analysis was performed to confirm the formation of the chlorinated compound and the drugs derivatives of CA. Confirmation of the successful chlorination of CA was achieved by recording its IR spectrum (Fig. 6). When comparing the spectrum of the resulting compound with the one of CA, a change in the broad absorption band belonging to the carboxylic acid group was observed within the range of (3300–3700) cm^{-1} . Additionally, there was a shift in the absorption signal associated with the carbonyl group from 1690 cm^{-1} to 1774 cm^{-1} . Such changes are indicator of the successful transformation of CA into its chlorinated derivative.

On the other hand, when comparing the spectrum of C-MET with the other spectra in Fig. 6, one can observe the characteristic group absorptions for the target compound. Starting with the band at 1263 cm^{-1} , it could be ascribed to C–O stretching in both CA and C-MET. Normally, this peak is absent in cinnamoyl chloride spectrum due to chlorination process. Again, carbonyl group at 1719 cm^{-1}

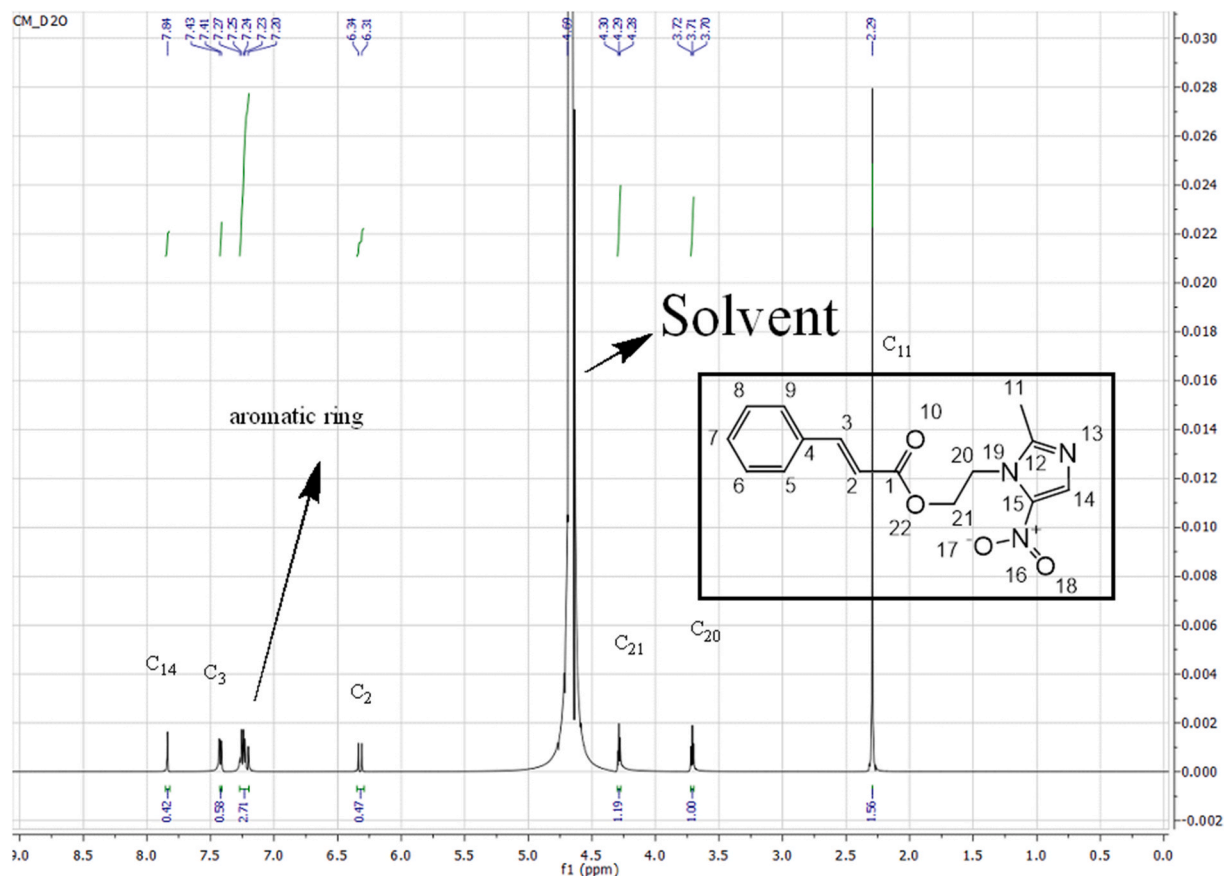


Fig. 7. ^1H NMR spectrum of C-MET.

Table 3

Chemical shift values and coupling constants for protons in C-MET compound.

Carbon atom number	^1H NMR (δ , ppm)	Signal style	Coupling constant (J, Hz)
11	2.29	Singlet 3H	–
20	3.71	Triplet 2H	5.3
21	4.28	Triplet 2H	5.3
2	6.31	Duplet 1H	16.2
Aromatic ring	7.2–7.3	Multiplet 5H	–
3	7.41	Duplet 1H	16.2
14	7.84	Singlet 1H	–

is the distinctive in confirming the esterification of CA and metronidazole as it shifted to a higher wavenumber in comparison with the acid and lower wave number in comparison with the chlorinated compound.

Peculiar absorbance bands were observed for C-MET at 2991 cm^{-1} for C–H stretching vibration of imidazole ring [21]. Also, symmetric and asymmetric stretching vibrations at 1365 and 1523 cm^{-1} were distinctive for N=O groups [22,23]. C-MEM derivative formation was confirmed by the occurrence of vibration bands comparable to specific amide bands at 1665 cm^{-1} , 1498 cm^{-1} , and 1290 cm^{-1} bands. The first band exemplifies the stretching vibrations of the C=O moiety (the lowest wavenumber of carbonyl group among all the four compounds), the second corresponds to –NH bending, and the third is because of –NH bending and C–N stretching of C–N–H functionalities. The spectrum also illustrates the typical band of amide –NH stretching at 3250 cm^{-1} [24]. Memantine portion is mainly represented by the C–H bond stretching at 2968 cm^{-1} [25,26].

3.2.2. NMR analysis

NMR spectrum is a powerful method to elucidate the derivative structure upon analysis of the chemical shifts and coupling constants. As per the recorded ^1H NMR spectrum using deuterated water as the solvent (Fig. 7), Table 3 illustrates the chemical shift values and coupling constants determined based on the instrument frequency of 600 MHz.

The ^1H NMR spectrum of C-MET manifested the characteristic proton singlet of –CH₃ on imidazole ring at δ 2.29 ppm (H-11) and

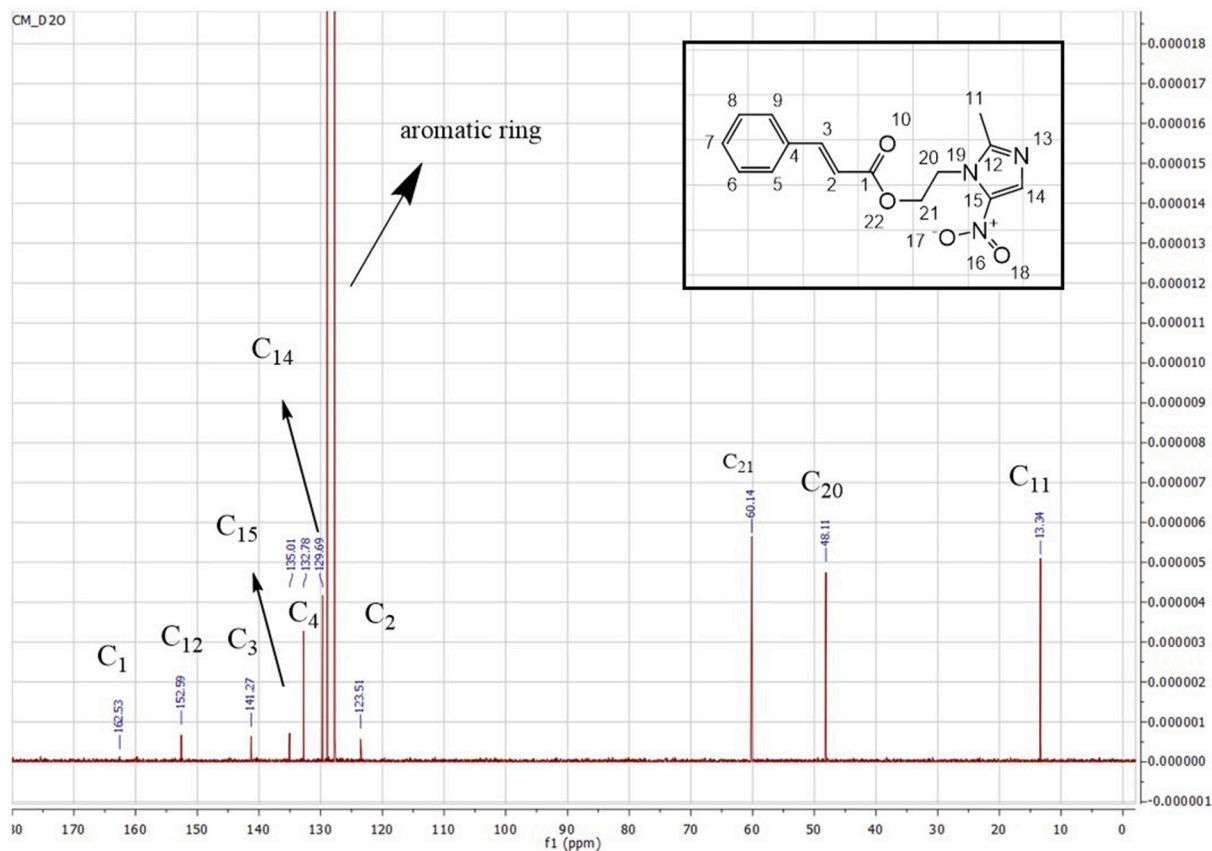


Fig. 8. ^{13}C NMR spectrum of C-MET.

Table 4

Chemical shift values and coupling constants for carbons in C-MEM compound.

Carbon atom number	^{13}C NMR (δ , ppm)
11	13.34
20	48.11
21	60.14
2	123.51
Aromatic ring	127.5–129
14	129.69
4	132.78
15	135.01
3	141.27
12	152.59
1	162.53

the triplets at δ 3.71 and 4.28 ppm (H-20 and 21, respectively) of ethyl group. On the other hand, CA moiety displayed several proton signals such as the doublet at δ 6.31 ppm (H-2) position, which could be ascribed to the methine group. Another important signal of CA is at δ 7.2–7.3 ppm as a multiplet of the aromatic ring. In short, the results of ^1H NMR analysis proved the successful reaction of the cinnamoyl portion with metronidazole. A similar conclusion was obtained as per the recorded ^{13}C NMR spectrum (Fig. 8) using deuterated water as the solvent, Table 4 illustrates the chemical shift values based on the instrument's frequency (600 MHz). The spectrum of C-MET is rich in detail, reflecting its complex structure. For CA, the signal at 162.53 ppm is characteristic of the carbonyl carbon, indicative of its electron-withdrawing nature and resonance effects within the molecule. The peaks at 141.27 ppm and 123.5 ppm are attributed to the vinylic carbons adjacent to the carbonyl group. The aromatic carbons resonate within a range of 127.5–129 ppm, typical for the delocalized electrons in the benzene ring. Finally, the signal at 132.78 ppm can be assigned to the carbon para to the carbonyl group, which is consistent with the expected chemical shift for such a position in an aromatic ring. For metronidazole, the methyl group on the imidazole ring, denoted as C11, resonates at 13.34 ppm. The signal at 152.59 ppm for C12 is indicative of a carbon

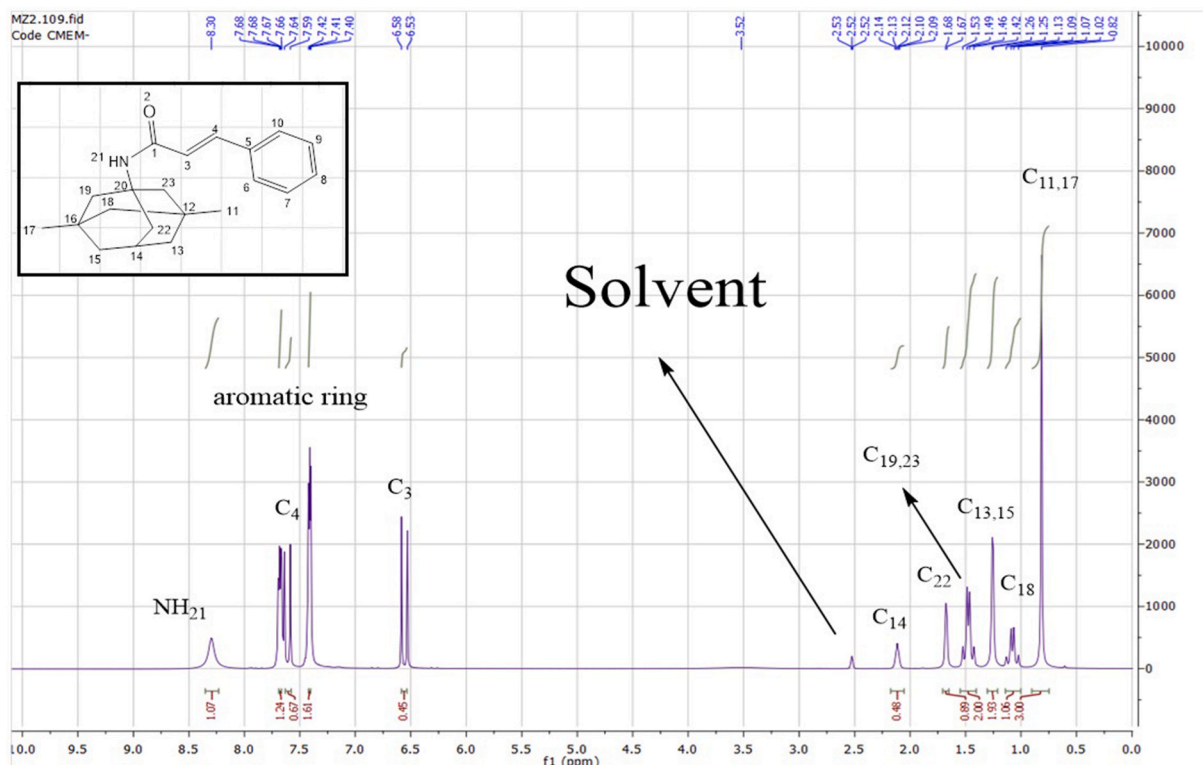


Fig. 9. ^1H NMR spectrum of C-MEM.

Table 5

Chemical shift values and coupling constants for protons in C-MEM compound.

Carbon atom number	^1H NMR (δ , ppm)	Signal style	Coupling constant (J, Hz)
11,17	0.82	Singlet 6H	–
18	1.08	Quartet 2H	$J_1 = 10.01$ $J_2 = 16.8$
13,15	1.255	Duplet 4H	$J_1 = 2.8$
19,23	1.48	Quartet 4H	$J_1 = 8.8$ $J_2 = 15.4$
22	1.675	Duplet 2H	$J_1 = 3.02$
14	2.12	Multiplet 1H	–
Aromatic ring	7.44–7.7	Multiplet 5H	–
3	6.55	Duplet 1H	16.1
4	7.66	Duplet 1H	16.1
(NH) 21	8.3	Singlet 1H	–

within the imidazole ring, suggesting deshielding due to the ring electronegativity. The hydroxyethyl side chain interacted with CA exhibited signals at 48.11 ppm and 60.14 ppm for C20 and C21, respectively; these shifts are consistent with a methylene group adjacent to an oxygen atom and a methylene group bonded to a nitrogen atom. Lastly, the signals at 129.69 ppm for C14 and 135.01 ppm for C15 are characteristic of carbons in a double bond, reflecting the electron-rich environment of the imidazole ring.

As per the recorded ^1H NMR spectrum (Fig. 9) using deuterated DMSO as the solvent, Table 5 illustrates the chemical shift values and coupling constants of C-MEM determined based on the instrument frequency (400 MHz). Spectral data analysis of chemical shifts manifested the characteristic proton singlet of the $-\text{NH}$ amidic group at δ 8.3 ppm (H-21) while other signals from H-11 to H-22 are ascribed to the methyl and methylene groups of memantine moiety. Again, the results of ^1H NMR analysis proved the successful amidation of cinnamoyl and memantine moieties. A similar conclusion was obtained as per the recorded ^{13}C NMR spectrum (Fig. 10) using deuterated water as the solvent, Table 6 illustrates the chemical shift values based on the instrument frequency (600 MHz). The chemical shifts and peaks of CA moiety are consistent with those observed in the C-MET compound, confirming the structural integrity of the cinnamic acid component. The memantine portion of the molecule exhibits a cluster of signals in the 29.55–52.83 ppm range, which correspond to the aliphatic carbons present in its structure. This range is typical for carbons in a saturated hydrocarbon environment.

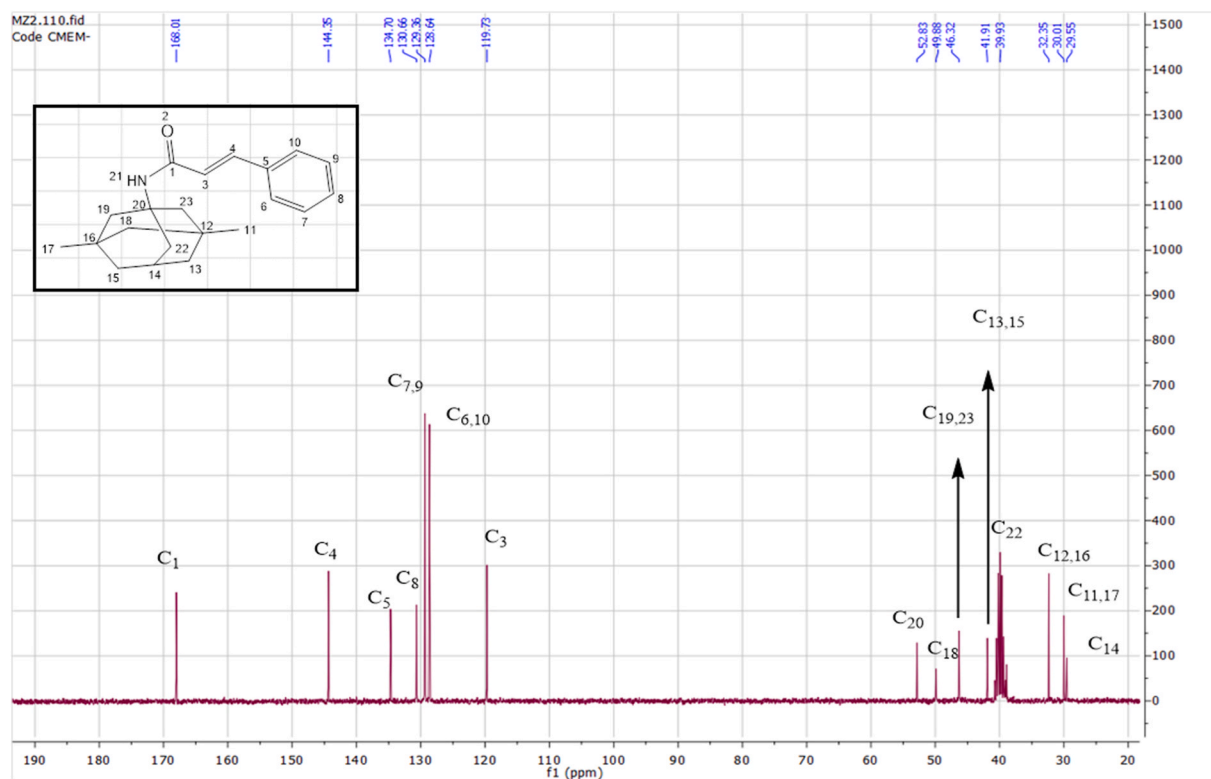


Fig. 10. ^{13}C NMR spectrum of C-MEM.

Table 6

Chemical shift values and coupling constants for carbons in C-MEM compound.

Carbon atom number	^{13}C NMR (δ , ppm)
14	29.55
11,17	30.01
12,16	32.35
22	39.93
13,15	41.91
19,23	46.32
18	49.88
20	52.83
3	119.73
6,10	128.64
7,9	129.36
8	130.66
5	134.7
4	144.35
1	168.01

3.3. Evaluation of the biological activity

The existence of antibacterial or antifungal efficacy was demonstrated through the observation of an inhibitory region surrounding the wells filled with the solution of the investigated substance. Measurement and subsequent expression in millimeters were carried out. The occurrence of antibacterial/antifungal activity was considered when the measured zone of inhibition exceeded 8 mm [27].

The antibacterial activity of metronidazole, memantine, CA, and the two derivatives (C-MET and C-MEM) were investigated against *S. aureus* and *P. aeruginosa*. From Fig. 11, it can be observed that there are no acceptable zones of inhibition for the pristine compounds (metronidazole, memantine, and CA) compared to the inhibition zone for the reference gentamicin in the $100\ \mu\text{g mL}^{-1}$ concentration for both types of bacteria. Although these compounds have been identified as agents with slight antibacterial activity, it seems that under the working concentrations, they were unable to illustrate any meaningful effect. On the other hand, the results indicate the importance of derivatization of such compounds. Comparatively, when measuring the diameter of the inhibition zones for the

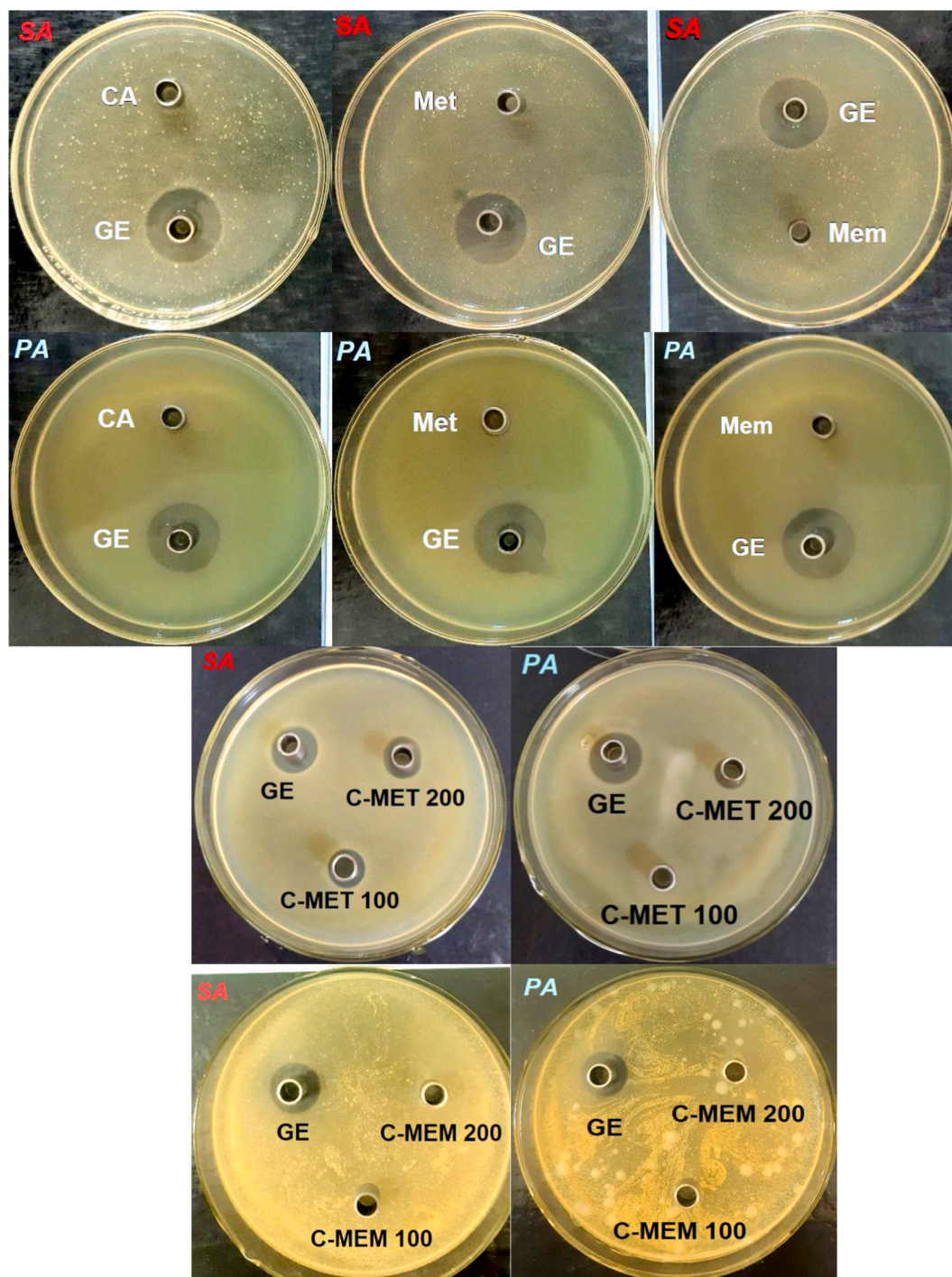


Fig. 11. The antibacterial effect pictures against *S. aureus* and *P. aeruginosa*.

derivatives samples, as shown in Table 7, it could be concluded that the synthesized compound (C-MET) exhibited considerable antimicrobial activity and was capable of inhibiting the growth of both bacteria with a superiority of activity on Gram-positive bacteria at the concentrations used. As for the compound C-MEM, as shown in Fig. 11 and compared to the inhibition zone for the reference substance (gentamicin), it is evident that it is not sufficiently capable of inhibiting the growth of the bacteria at the concentrations used. Therefore, the compound is not considered to possess biological activity, as indicated in Table 7 (8 mm at 100 and 200 $\mu\text{g mL}^{-1}$).

The antifungal activity of the compounds was examined against the fungi *Candida albicans*. Opposite to antibacterial activity, it can be observed from Fig. 12 that there are no zones of inhibition for the compound C-MET compared to the inhibition zone for the

Table 7
Inhibition zone diameters for gentamicin and the derivatives against tested bacteria.

	Diameter of the inhibition zone (mm)					
	DMSO	Gentamicin	C-MET		C-MEM	
$\mu\text{g.mL}^{-1}$	-	100	100	200	100	200
G+	-	17	12	15	8	8
G-	-	18	8	11	8	8

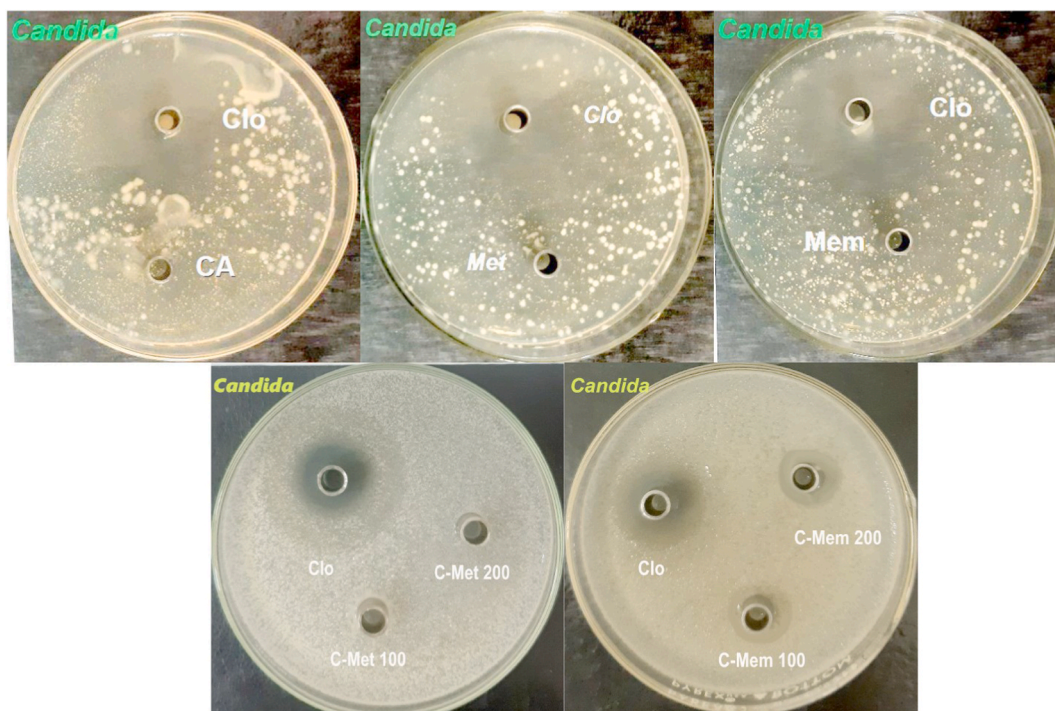


Fig. 12. The antifungal effect pictures against *Candida albicans*.

Table 8
Inhibition zone diameters for clotrimazole and the derivatives against tested fungus.

	Diameter of the inhibition zone (mm)					
	DMSO	Clotrimazole	C-MET		C-MEM	
$\mu\text{g.mL}^{-1}$	-	100	100	200	100	200
Candida	-	21	8	8	11	14

reference substance (clotrimazole). By measuring the diameter of the inhibition zones for the samples, as shown in Table 8, it can be concluded that the compound C-MET is inactive and does not have a tendency to inhibit the growth of *Candida* at the concentrations used. Whereas coupling of CA and memantine proved to have a positive effect on the antifungal property of the compound, as shown in Fig. 12, and compared to the inhibition zone for the reference substance, it is evident that there is respectful inhibition zones for C-MEM. Bare samples have also shown no effective antifungal activities as no inhibition zones were observed.

Metronidazole is known as a potent anti-anaerobic drug and well-known as ineffective to aerobic bacteria. However, it seems that as a hybrid with CA, it worked well against Gram-positive bacteria. This result suggests that the C-MET derivative has changed the metronidazole mechanism of action for unknown reasons. This interpretation is in agreement with earlier observations provided by Zhou *et al.* that nitroimidazoles conjugated with an indolin-2-one substituent demonstrated exceptional, submicromolar potency in eradicating aerobically growing bacteria [28]. It was then evident by Reinhardt *et al.* that nitroimidazole derivatives inhibited topoisomerase IV as a primary antibiotic target in pathogenic *Staphylococcus aureus* which fits well to our results [29]. Furthermore, C-MEM has only shown antifungal activity. So, one can say that a synergistic effect has taken place between the two components rather than a change in the mechanism of action. It should be noted that bacterial cell membrane permeability is affected by ion loss and membrane potential reduction. This damage can lead to macromolecules penetrating and ultimately result in bacterial death.

Therefore, it is possible to postulate that certain samples [30].

4. Conclusions

Two derivatives were synthesized from cinnamic acid with the pharmaceutical compounds (metronidazole and memantine) through two steps and two different methods. The appropriate reaction conditions were applied to achieve the best yield of the chemical reactions and the structures of intermediate compounds and the final products were confirmed employing FT-IR, ^1H NMR, and ^{13}C NMR). The effectiveness of the resulting compounds against both Gram -positive and -negative bacteria and fungi, was evaluated compared to gentamicin and clotrimazole as active reference compounds. Only the compound (C-MET) showed satisfactory results against the Gram -positive bacteria. Here, we demonstrated for the first time a derivative containing metronidazole to be active against aerobic bacteria. Furthermore, only the compound (C-MEM) showed satisfactory antifungal results where it could be concluded that memantine was capable of synergistically enhancing the antibacterial activity of CA against fungal cells.

In summary, our study provides a foundation for future research aimed at developing potent antimicrobial agents. Investigating structural modifications to fine-tune the compounds interactions with bacterial and fungal targets via rational design based on molecular modeling would be a great asset in this regard. By refining these derivatives and exploring novel strategies, we can contribute to the fight against infectious diseases.

Data availability

Data will be made available on request.

CRedit authorship contribution statement

Mohammad Moatz Shollar: Writing – original draft, Methodology, Investigation. **Joumaa Merza:** Validation, Supervision, Formal analysis. **Maher Darwish:** Writing – review & editing, Validation, Software, Formal analysis. **Mohammad Keshe:** Visualization, Software, Conceptualization.

Declaration of generative AI and AI-assisted technologies in the writing process

During the preparation of this work the authors used copilot in order to improve language and readability. After using this tool/service, the authors reviewed and edited the content as needed and take full responsibility for the content of the publication.

Declaration of competing interest

The authors declare that they have no known competing financial interests or personal relationships that could have appeared to influence the work reported in this paper.

Acknowledgements

The authors wish to thank the Faculty of Science, Al-Baath University for the financial and instrumental support of this research.

References

- [1] K.R. Campos, P.J. Coleman, J.C. Alvarez, S.D. Dreher, R.M. Garbaccio, N.K. Terrett, R.D. Tillyer, M.D. Truppo, E.R. Parmee, The importance of synthetic chemistry in the pharmaceutical industry, *Science* 363 (6424) (2019) eaat0805.
- [2] D. Insuasty, J. Castillo, D. Becerra, H. Rojas, R. Abonia, Synthesis of biologically active molecules through multicomponent reactions, *Molecules* 25 (3) (2020) 505–576.
- [3] W.J. Watson, Chemical process research: the art of practical synthesis, in: Ahmed F. Abdel-Magid, John A. Ragan (Eds.), ACS Symposium Series 870. American Chemical Society: Washington, DC, 2004, p. 211, pp., *Org. Process Res. Dev.* 8(6) (2004) 1086–1086.
- [4] J.A.d. Vale, M.P. Rodrigues, Á.M.A. Lima, S.S. Santiago, G.D.d.A. Lima, A.A. Almeida, L.L.d. Oliveira, G.C. Bressan, R.R. Teixeira, M. Machado-Neves, Synthesis of cinnamic acid ester derivatives with antiproliferative and antimetastatic activities on murine melanoma cells, *Biomed. Pharmacother.* 148 (2022) 112689.
- [5] N. Ruwizhi, B.A. Aderibigbe, Cinnamic acid derivatives and their biological efficacy, *Int. J. Mol. Sci.* 21 (16) (2020) 5712.
- [6] P. Su, Y. Shi, J. Wang, X. Shen, J. Zhang, Anticancer agents derived from natural cinnamic acids, *Anti Cancer Agents Med. Chem.* 15 (8) (2015) 980–987.
- [7] S. Huang, W. Liu, Y. Li, K. Zhang, X. Zheng, H. Wu, G. Tang, Design, synthesis, and activity study of cinnamic acid derivatives as potent antineuroinflammatory agents, *ACS Chem. Neurosci.* 12 (3) (2021) 419–429.
- [8] E. Indriyanti, M.S. Prahasiwi, Synthesis of cinnamic acid based on Perkin reaction using sonochemical method and its potential as photoprotective agent, *JKPK* 5 (1) (2020) 8.
- [9] E. Scott, F. Peter, J. Sanders, Biomass in the manufacture of industrial products—the use of proteins and amino acids, *Appl. Microbiol. Biotechnol.* 75 (4) (2007) 751–762.
- [10] M. Sova, Antioxidant and antimicrobial activities of cinnamic acid derivatives, *Mini-Rev. Med. Chem.* 12 (8) (2012) 749–767.
- [11] B. Korošec, M. Sova, S. Turk, N. Kraševc, M. Novak, L. Lah, J. Stojan, B. Podobnik, S. Berne, N. Zupanec, M. Bunc, S. Gobec, R. Komel, Antifungal activity of cinnamic acid derivatives involves inhibition of benzoate 4-hydroxylase (CYP53), *J. Appl. Microbiol.* 116 (4) (2014) 955–966.
- [12] M.P. Rodrigues, D.C. Tomaz, L. Ângelo de Souza, T.S. Onofre, W. Aquiles de Menezes, J. Almeida-Silva, A.M. Suarez-Fontes, M. Rogéria de Almeida, A. Manoel da Silva, G.C. Bressan, M.A. Vannier-Santos, J.L. Rangel Fietto, R.R. Teixeira, Synthesis of cinnamic acid derivatives and leishmanicidal activity against *Leishmania braziliensis*, *Eur. J. Med. Chem.* 183 (2019) 111688.

- [13] M. Naveed, V. Hejazi, M. Abbas, A.A. Kamboh, G.J. Khan, M. Shumzaid, F. Ahmad, D. Babazadeh, X. FangFang, F. Modarresi-Ghazani, L. WenHua, Z. XiaoHui, Chlorogenic acid (CGA): a pharmacological review and call for further research, *Biomed. Pharmacother.* 97 (2018) 67–74.
- [14] Y. Wang, F. He, S. Wu, Y. Luo, R. Wu, D. Hu, B. Song, Design, synthesis, anti-TMV activity, and preliminary mechanism of cinnamic acid derivatives containing dithioacetal moiety, *Pestic. Biochem. Physiol.* 164 (2020) 115–121.
- [15] M. Toolabi, S. Moghimi, T.O. Bakhshaesh, S. Salarinejad, A. Aghcheli, Z. Hasanvand, E. Nazeri, A. Khalaj, R. Esmaili, A. Foroumadi, 6-Cinnamoyl-4-arylaminothienopyrimidines as highly potent cytotoxic agents: design, synthesis and structure-activity relationship studies, *Eur. J. Med. Chem.* 185 (2020) 111786.
- [16] S. Ghafary, Z. Najafi, M. Mohammadi-Khanaposhtani, H. Nadri, N. Edraki, N. Ayashi, B. Larijani, M. Amini, M. Mahdavi, Novel cinnamic acid–tryptamine hybrids as potent butyrylcholinesterase inhibitors: synthesis, biological evaluation, and docking study, *Arch. Pharm.* 351 (10) (2018) 1800115.
- [17] M. Mohammed, N. Haj, Synthesis and pharmacological characterization of metronidazole-oxadiazole derivatives, *Iran. J. Med. Sci.* 48 (2) (2023) 167–175.
- [18] A. Tencheva, I. Stankova, T. Angelova, V. Nemska, N. Georgieva, D. Danalev, Antimicrobial activity of amino acid derivatives of memantine, *J. Chem. Technol. Metall.* 57 (2) (2022) 286–290.
- [19] https://www.oc-praktikum.de/nop/en/instructions/pdf/2013_en.pdf.
- [20] H.A. Khdera, S.Y. Saad, A. Moustapha, F. Kandil, Synthesis of new flavonoid derivatives based on 3-hydroxy-4'-dimethylamino flavone and study the activity of some of them as antifungal, *Heliyon* 8 (12) (2022) e12062.
- [21] D. Kathyayani, B. Mahesh, D. Channe Gowda, A. Sionkowska, S. Veeranna, Investigation of miscibility and physicochemical properties of synthetic polypeptide with collagen blends and their wound healing characteristics, *Int. J. Biol. Macromol.* 246 (2023) 125704.
- [22] M. Trivedi, S. Patil, H. Shettigar, K. Bairwa, S. Jana, Spectroscopic characterization of biofield treated metronidazole and tinidazole, *Med. Chem.* 7 (5) (2015) 340–344.
- [23] Z. Feyissa, G.D. Edossa, N.K. Gupta, D. Negera, Development of double crosslinked sodium alginate/chitosan based hydrogels for controlled release of metronidazole and its antibacterial activity, *Heliyon* (2023) e20144.
- [24] B. Mahesh, H.R. Lokesh, D. Kathyayani, A. Sionkowska, D.C. Gowda, K. Adamiak, Interaction between synthetic elastin-like polypeptide and collagen: Investigation of miscibility and physicochemical properties, *Polymer* 272 (2023) 125833.
- [25] S. Ganguly, T. Maity, S. Mondal, P. Das, N.C. Das, Starch functionalized biodegradable semi-IPN as a pH-tunable controlled release platform for memantine, *Int. J. Biol. Macromol.* 95 (2017) 185–198.
- [26] V. Rani, R. Verma, K. Kumar, R. Chawla, pH-influenced self-assembled stealth nanoscaffolds encapsulating memantine for treatment of Alzheimer's disease, *J. Biosci.* 48 (3) (2023) 31–55.
- [27] A. Jitareanu, G. Tatarina, A. Zbancioc, C. Tuchilus, M. Balan, U. Stanescu, Cinnamic acid derivatives and 4-aminoantipyrine amides—synthesis and evaluation of biological properties, *Res. J. Chem. Sci.* 2231 (2013) 606X.
- [28] Y. Zhou, Y. Ju, Y. Yang, Z. Sang, Z. Wang, G. He, T. Yang, Y. Luo, Discovery of hybrids of indolin-2-one and nitroimidazole as potent inhibitors against drug-resistant bacteria, *J. Antibiot.* 71 (10) (2018) 887–897.
- [29] T. Reinhardt, K.M. Lee, L. Niederegger, C.R. Hess, S.A. Sieber, Indolin-2-one nitroimidazole antibiotics exhibit an unexpected dual mode of action, *ACS Chem. Biol.* 17 (11) (2022) 3077–3085.
- [30] B. Roopashree, B. Mahesh, R. Ramu, N.D. Rekha, S.N. Manjula, G. Preethi, V. Gayathri, An insight into the cytotoxic, antimicrobial, antioxidant, and biocontrol perspective of novel Iron(III) complexes of substituted benzimidazoles: inhibition kinetics and molecular simulations, *J. Biomol. Struct. Dyn.* 4 (2023) 1–17.